

---

# JINA-CLIP-V2: MULTILINGUAL MULTIMODAL EMBEDDINGS FOR TEXT AND IMAGES

Andreas Koukounas\* Georgios Mastrapas\* Bo Wang Mohammad Kalim Akram  
 Sedigheh Eslami Michael Günther Isabelle Mohr Saba Sturua Scott Martens  
 Nan Wang Han Xiao

Jina AI GmbH,  
 Prinzessinnenstr. 19-20, 10969  
 Berlin, Germany  
 research@jina.ai

## ABSTRACT

Contrastive Language-Image Pretraining (CLIP) is a highly effective method for aligning images and texts in a shared embedding space. These models are widely used for tasks such as cross-modal information retrieval and multi-modal understanding. However, CLIP models often struggle with text-only tasks, underperforming compared to specialized text models. This performance disparity forces retrieval systems to rely on separate models for text-only and multi-modal tasks. In this work, we build upon our previous model, `jina-clip-v1`, by introducing a refined framework that utilizes multi-task, multi-stage contrastive learning across multiple languages, coupled with an improved training recipe to enhance text-only retrieval. The resulting model, `jina-clip-v2`, outperforms its predecessor on text-only and multimodal tasks, while adding multilingual support, better understanding of complex visual documents and efficiency gains thanks to Matryoshka Representation Learning and vector truncation. The model performs comparably to the state-of-the-art in both multilingual-multimodal and multilingual text retrieval benchmarks, addressing the challenge of unifying text-only and multi-modal retrieval systems.

## 1 INTRODUCTION

Contrastive text-image pre-training has become a widely adopted approach to building robust text-image alignment models. These models are particularly effective for tasks like cross-modal retrieval and zero-shot classification (Radford et al., 2021), demonstrating strong generalization capabilities. Conventional text-image pre-training excels at aligning text and image embeddings but struggles with aligning text-to-text embeddings (Koukounas et al., 2024). This is because cross-modal retrieval training is inadequate for text-only retrieval. The texts available are typically image captions, which are generally short and information-poor, and training procedures don't use standard techniques for training text embeddings, like hard negatives. (Zhang et al., 2024a)

To overcome these limitations, Koukounas et al. (2024) introduced a multi-task, multi-stage contrastive learning approach to simultaneously align text-text and text-image embeddings. Their method involves three stages: optimizing text-text and text-image embeddings for short image-caption and text-text pairs (stage 1), refining alignment using long text-text pairs and detailed image-caption pairs (stage 2) and further enhancing performance with text triplets containing hard negatives and detailed image-caption pairs (stage 3). The resulting model, `jina-clip-v1`, achieves strong performance on both the cross-modal CLIP Benchmark<sup>1</sup> and text embedding MTEB Benchmark (Muennighoff et al., 2023).

Despite its strengths, this model has several limitations. First, it is an English-only multi-modal embedding model, which makes it unsuitable for multilingual document retrieval. Second,

---

\*Equal contribution

<sup>1</sup>[https://github.com/LAION-AI/CLIP\\_benchmark](https://github.com/LAION-AI/CLIP_benchmark)

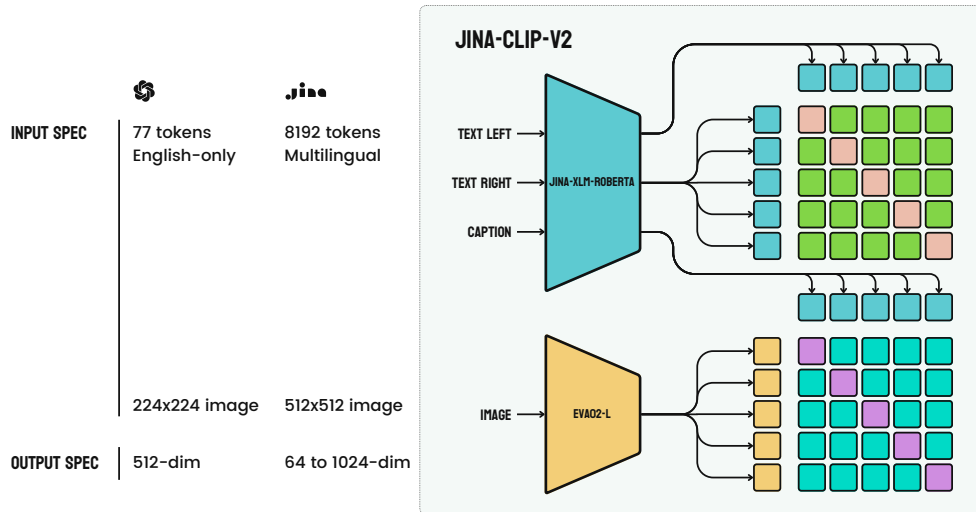


Figure 1: `jina-clip-v2` combines a text encoder (Jina XLM-RoBERTa, 561M parameters) and a vision encoder (EVA02-L14, 304M parameters) for a total of 865M parameters. The text encoder is also used in `jina-embeddings-v3`.

`jina-clip-v1` struggles with images that contain text, tables, graphs, diagrams, and other complex content (Faysse et al., 2024).

To address these challenges, we propose an enhanced text-image pre-training scheme. Our approach incorporates multilingual text-image and text-text pairs, along with text-image pairs containing text and other difficult-to-process complex visual structures. Additionally, we gradually increase image resolution during pre-training to balance computational efficiency and model performance. The resulting model, `jina-clip-v2` depicted in Figure 1, not only achieves competitive performance on cross-modal retrieval benchmarks against state-of-the-art models like NLLB-CLIP-SigLIP (Vishratin, 2023b) but also performs comparably to dedicated multilingual text embedding models like `jina-embeddings-v3` (Sturua et al., 2024) on the Retrieval and STS tasks of the multilingual MTEB benchmark (Muennighoff et al., 2023). Moreover, due to the inclusion of visually rich training data and the progressive increase in image resolution, `jina-clip-v2` demonstrates significantly improved performance on benchmarks for visually rich document retrieval, compared to `jina-clip-v1`. To reduce vector storage costs, we employ Matryoshka Representation Learning (Kusupati et al., 2024) to enable dimension truncation on the output vectors with minimal performance degradation.

## 2 RELATED WORK

Radford et al. (2021) pioneered the dual encoder architecture trained contrastively on image-text pairs, demonstrating impressive zero-shot performance and laying the groundwork for pre-trained vision-language models. Building upon this foundation, Zhai et al. (2023) propose an alternative and more efficient sigmoid objective, while Sun et al. (2023) optimize the model’s dimensions and scale up both dataset and model sizes, achieving state-of-the-art performance on cross-modal tasks. Koukounas et al. (2024) enhance a CLIP-based retriever with strong text-to-text and cross-modal retrieval capabilities, though fall short in addressing retrieval scenarios that involve candidate pools with heterogeneous modalities, due to the modality gap (Liang et al., 2022). To mitigate the modality bias, Lin et al. (2024) take a different approach by fine-tuning a multimodal LLM with modality-aware hard-negative mining, creating a universal multimodal retriever and maintaining competitive text-to-text retrieval performance across diverse tasks.

Extensive research has also focused on extending CLIP’s capabilities to multilingual contexts. To address the lack of image-caption pairs in languages other than English, Carlsson et al. (2022)

Table 1: Model properties

Feature	Text Encoder	Image Encoder
Base Model	Jina-XLM-RoBERTa (Sturua et al., 2024)	EVA02 L/14 (Sun et al., 2023)
Parameters	561M	304M
Input Specification	8,192 tokens (max)	512x512 pixels
Output Dimensions	1,024	1,024
Layers	24	24
Attention Implementation	FlashAttention2 (Dao et al., 2022)	xFormers (Lefaudeux et al., 2022)
Pooling Strategy	Mean pooling	CLS pooling
Additional Features	89 languages supported	Patch size 14x14

apply knowledge distillation to retrain the text encoder using machine translation data. NLLB-CLIP (Visheratin, 2023a) leverages Locked-image Tuning (LiT) (Zhai et al., 2022) alongside the NLLB (Costa-jussà et al., 2022) text encoder, achieving state-of-the-art results in both retrieval and classification tasks.

The importance of good information retrieval in Retrieval-Augmented Generation (RAG) systems has motivated rapid progress in multilingual text embedding models. These models are typically based on either a robust encoder-only architecture, such as XLM-RoBERTa (Conneau et al., 2020) or a decoder-only multilingual large language model, such as Mistral 7B (Jiang et al., 2023). Multilingual E5 (Wang et al., 2024) and BGE-M3 (Chen et al., 2024) both use XLM-RoBERTa as their backbone, leveraging extensive multilingual training with instruction tuning and multi-task learning techniques, respectively. mGTE (Zhang et al., 2024b) achieves comparable performance to BGE-M3 using a smaller transformer architecture, enhanced by RoPE (Su et al., 2023) to extend the context length. Similarly, Sturua et al. (2024) employ RoPE to increase the model’s context length and apply LoRA tuning (Hu et al., 2021) to optimize embeddings for downstream tasks.

### 3 TRAINING

The `jina-clip-v2` model uses the dual encoder architecture, introduced in the original CLIP (Radford et al., 2021) model and reused in `jina-clip-v1` (Koukounas et al., 2024). One encoder is responsible for encoding texts in a 1024-dimensional embedding space, while a second encoder embeds images in the same embedding space.

The text encoder is initialized with the pre-trained Jina-XLM-RoBERTa model weights. Introduced in `jina-embeddings-v3` (Sturua et al., 2024), the Jina-XLM-RoBERTa model is a port of the XLM-RoBERTa (Conneau et al., 2020) weights to a modern encoder-only architecture that adds Flash Attention (Dao et al., 2022), rotary positional embeddings (Su et al., 2023) and LoRA (Hu et al., 2021).

For the image encoder, we have opted for the EVA02 (Fang et al., 2023b) family of ViT models, similarly to `jina-clip-v1`. We have selected a relatively large pre-trained model, similar in size to the text encoder. This model implementation includes 2D rotary positional embeddings (Su et al., 2023) and a memory-efficient attention implementation based on xFormers (Lefaudeux et al., 2022).

Architectural details for both encoders are presented in Table 1.

#### 3.1 DATASETS

Similarly to `jina-clip-v1` (Koukounas et al., 2024), we construct four different training datasets. Dataset  $\mathbb{D}^{\text{txt};\text{p}}$  denotes a dataset of text pairs,  $\mathbb{D}^{\text{txt};\text{t}}$  denotes a dataset of text samples with hard negatives,  $\mathbb{D}^{\text{mm};\text{s}}$  a multimodal short-caption dataset and  $\mathbb{D}^{\text{mm};\text{l}}$  a multimodal long-caption dataset. All datasets are multi-lingual.

The text corpora  $\mathbb{D}^{\text{txt};\text{p}}$  and  $\mathbb{D}^{\text{txt};\text{t}}$  are introduced in Sturua et al. (2024) and contain data in 30 languages. The text pair corpus  $\mathbb{D}^{\text{txt};\text{p}}$  consists of query and target pairs from a diverse collection of text-pair datasets. The triplet text corpus  $\mathbb{D}^{\text{txt};\text{t}}$  is a high-quality dataset with hard negatives from various sources. Each training item contains one annotated positive and seven negative items.

---

Regarding  $\mathbb{D}^{\text{txt};t}$ , we focus on Retrieval and Semantic Textual Similarity (STS) datasets for the scope of this work.

Our multi-modal training data comes from multiple sources. For the English part, we rely on the DFN dataset (Fang et al., 2023a), a collection of  $\sim 400\text{M}$  image-caption pairs, filtered using data filtering networks. For the rest of the languages, we collect  $\sim 400\text{M}$  samples from CommonPool (Gadre et al., 2023), using multilingual CLIP to identify and discard low-quality items. All images are resized to (384, 384). These two large-scale datasets are included in  $\mathbb{D}^{\text{mm};s}$  and a small part with captions longer than 256 tokens is held out for  $\mathbb{D}^{\text{mm};l}$ .

Inspired by visual QA applications (Faysse et al., 2024), We have diversified our training data with PDFs, scientific graphs, infographics and Wikipedia images. The following datasets are included in both  $\mathbb{D}^{\text{mm};s}$  and  $\mathbb{D}^{\text{mm};l}$ : DocVQA (Mathew et al., 2021b), TatDQA (Zhu et al., 2022), InfographicsVQA (Mathew et al., 2021a), SciGraphQA (Li & Tajbakhsh, 2023), ArXivQA and ArXivCAP (Li et al., 2024), WIT (Srinivasan et al., 2021) and ViDoRe synthetic training data (Faysse et al., 2024). For the QA datasets, to obtain a caption for an image, we concatenate query and answer for each sample. For the WIT dataset, we use the reference caption in  $\mathbb{D}^{\text{mm};s}$  and a concatenation of caption, page title, section title, page description and section description for  $\mathbb{D}^{\text{mm};l}$ .

Finally,  $\mathbb{D}^{\text{mm};l}$  includes multilingual synthetic long captions, similar to how Koukounas et al. (2024) make use of ShareGPT4v (Chen et al., 2023a). We use the GPT4v API (OpenAI, 2023) to generate detailed image descriptions for 40,000 images in 30 languages. This adds 1.2M generated multilingual long captions to  $\mathbb{D}^{\text{mm};l}$ .

### 3.2 TRAINING STAGES

Following the strategy proposed in Koukounas et al. (2024), we employ a multi-task, multi-stage training approach, in order to optimize the model for two tasks simultaneously: text-image matching and text-text matching.

**Stage 1** focuses on aligning the multi-modal representations while also improving the text representations of the text encoder. We train on  $\mathbb{D}^{\text{txt};p}$  and  $\mathbb{D}^{\text{mm};s}$ , with a small context length of 77 and an image resolution of (224, 224) to enable large batch sizes. Towards the end, when performance peaks, we switch to a higher image resolution of (384, 384) using positional embedding interpolation as a warm-up for the next stage.

**Stage 2** trains on  $\mathbb{D}^{\text{txt};p}$  and  $\mathbb{D}^{\text{mm};l}$ , with context length increased from 77 to 512 and image resolution set at (384, 384). This stage improves text embedding performance on longer text lengths, while maintaining alignment between the two modalities.

**Stage 3** uses hard negatives from  $\mathbb{D}^{\text{txt};t}$  to further improve the text encoder in distinguishing relevant from irrelevant text. To maintain text-image alignment, we continue training with  $\mathbb{D}^{\text{mm};l}$ . We do one more positional embedding interpolation to increase the image resolution to (512, 512) and train on this resolution for the duration of stage 3.

Appendix table 6 specifies the training details for each step.

### 3.3 LOSS FUNCTIONS

Given a batch  $\mathbf{B} \subset \mathbb{D}^{\text{pairs}}$  of embedding pairs  $(\mathbf{q}, \mathbf{p})$ , the InfoNCE loss  $\mathcal{L}_{\text{nce}}$  (Van den Oord et al., 2018), given in equation 1, evaluates the cosine similarity  $\text{cos}(\mathbf{q}, \mathbf{p})$  between query  $q$  and its corresponding target  $p$ , relative to the similarity of all other targets in the batch. The loss is calculated in both directions to preserve the symmetry of similarity measures. The temperature parameter  $\tau$

influences how the loss function weighs minor differences in the similarity scores.

$$\begin{aligned}
\mathcal{L}_{\text{nce}}(\mathbf{B}) &:= \mathcal{L}_{\text{nce}}^{\rightarrow}(\mathbf{B}) + \mathcal{L}_{\text{nce}}^{\leftarrow}(\mathbf{B}), \text{ with} \\
\mathcal{L}_{\text{nce}}^{\rightarrow}(\mathbf{B}) &:= \mathbb{E}_{(\mathbf{q}, \mathbf{p}) \sim \mathbf{B}} \left[ -\ln \frac{e^{\cos(\mathbf{q}, \mathbf{p})/\tau}}{\sum_{i=1}^k e^{\cos(\mathbf{q}, \mathbf{p}_i)/\tau}} \right] \\
\mathcal{L}_{\text{nce}}^{\leftarrow}(\mathbf{B}) &:= \mathbb{E}_{(\mathbf{q}, \mathbf{p}) \sim \mathbf{B}} \left[ -\ln \frac{e^{\cos(\mathbf{p}, \mathbf{q})/\tau}}{\sum_{i=1}^k e^{\cos(\mathbf{p}, \mathbf{q}_i)/\tau}} \right]
\end{aligned} \tag{1}$$

When hard negatives are available for query  $q$ , an extended version of the  $\mathcal{L}_{\text{nce}}$  loss is used. Given a batch  $\mathbf{B} \subset \mathbb{D}^{\text{triplets}}$  of samples  $(\mathbf{q}, \mathbf{p}, \mathbf{n}_1, \dots, \mathbf{n}_7)$ , consisting of a query  $\mathbf{q}$ , a positive match  $\mathbf{p}$ , and seven negatives  $\mathbf{n}_1, \dots, \mathbf{n}_7$ , the extended loss function, denoted here as  $\mathcal{L}_{\text{nce}^+}$ , is given in equation 2. Similarly to  $\mathcal{L}_{\text{nce}}$ , this loss function is bidirectional.

$$\begin{aligned}
\mathcal{L}_{\text{nce}^+}(\mathbf{B}) &:= \\
&\mathbb{E}_{r \sim \mathbf{B}} \left[ -\ln \frac{e^{\cos(\mathbf{q}, \mathbf{p})/\tau}}{\sum_{i=1}^k \left[ e^{\cos(\mathbf{q}, \mathbf{p}_i)/\tau} + \sum_{j=1}^7 e^{\cos(\mathbf{q}, \mathbf{n}_{j,i})/\tau} \right]} \right] \\
&+ \mathbb{E}_{r \sim \mathbf{B}} \left[ -\ln \frac{e^{\cos(\mathbf{p}, \mathbf{q})/\tau}}{\sum_{i=1}^k e^{\cos(\mathbf{p}, \mathbf{q}_i)/\tau}} \right] \\
&\text{with } r = (\mathbf{q}, \mathbf{p}, \mathbf{n}_1, \dots, \mathbf{n}_7).
\end{aligned} \tag{2}$$

Equation 3 formulates the loss for each of the three stages. In each stage, we optimize a joint loss function, i.e. the sum of two loss functions, one operating on text representations and one on multi-modal representations. All stages optimize  $\mathcal{L}_{\text{nce}}$  except Stage 3, which uses hard negatives in the text loss branch and thus calculates  $\mathcal{L}_{\text{nce}^+}$ .

$$\begin{aligned}
\mathcal{L}_1(\mathbf{B}_{\text{txt};p}, \mathbf{B}_{\text{mm};s}) &:= \mathcal{L}_{\text{nce}}(\mathbf{B}_{\text{txt};p}) + \mathcal{L}_{\text{nce}}(\mathbf{B}_{\text{mm};s}) \\
\mathcal{L}_2(\mathbf{B}_{\text{txt};p}, \mathbf{B}_{\text{mm};l}) &:= \mathcal{L}_{\text{nce}}(\mathbf{B}_{\text{txt};p}) + \mathcal{L}_{\text{nce}}(\mathbf{B}_{\text{mm};l}) \\
\mathcal{L}_3(\mathbf{B}_{\text{txt};t}, \mathbf{B}_{\text{mm};l}) &:= \mathcal{L}_{\text{nce}^+}(\mathbf{B}_{\text{txt};t}) + \mathcal{L}_{\text{nce}}(\mathbf{B}_{\text{mm};l})
\end{aligned} \tag{3}$$

In Equation 3,  $\mathbf{B}_{\text{txt};p} \subset \mathbb{D}^{\text{txt};p}$  denotes a batch of text pairs drawn from the dataset of text pairs  $\mathbb{D}^{\text{txt};p}$ , while  $\mathbf{B}_{\text{txt};t} \subset \mathbb{D}^{\text{txt};t}$  denotes a batch of text samples with negatives drawn from the hard negatives dataset  $\mathbb{D}^{\text{txt};t}$ . Similarly  $\mathbf{B}_{\text{mm};s} \subset \mathbb{D}^{\text{mm};s}$  denotes a batch of text-image pairs drawn from the multimodal short-caption dataset  $\mathbb{D}^{\text{mm};s}$ , while  $\mathbf{B}_{\text{mm};l} \subset \mathbb{D}^{\text{mm};l}$  denotes a batch of text-image pairs sampled from the multimodal long-caption dataset  $\mathbb{D}^{\text{mm};l}$ .

### 3.4 MATRYOSHKA REPRESENTATION LEARNING

In all stages of training, each loss function is evaluated on the full 1024-dimension output vectors of the two encoders as well as on truncated vectors of 64, 128, 256, 512 and 768 dimensions. In other words, each loss component  $\mathcal{L}$  on equation 3 is the sum of the same loss function evaluated at different embedding dimensionalities.

This training technique, called *Matryoshka Representation Learning*, (Kusupati et al., 2024) trains the model to learn the most important features in the vector sequence. This makes it possible, at inference time, to truncate embedding vectors, thereby reducing storage and computation costs when comparing vectors, at a minor performance penalty.

Table 2: Evaluation results on cross-modal tasks

Benchmark	CLIP Benchmark - EN		Crossmodal-3600		Multilingual MS COCO	
Task Type	Zero-Shot Retrieval					
Model - Metric	T-I r@5	I-T r@5	T-I r@5	I-T r@5	T-I r@5	I-T r@5
nllb-siglip-large	<b>81.54</b>	88.15	82.07	80.16	<b>87.60</b>	85.37
nllb-siglip-base	79.57	86.38	79.29	76.56	86.23	84.87
jina-clip-v1	77.75	87.65	-	-	-	-
jina-clip-v2stage 1	73.87	86.61	73.51	79.64	80.66	83.02
jina-clip-v2stage 2	79.81	89.57	<b>84.13</b>	<b>84.12</b>	86.11	<b>86.45</b>
jina-clip-v2	79.09	<b>89.73</b>	81.43	83.23	84.87	86.03

T-I r@5 : Text to Image Recall@5 [%]    I-T r@5 : Image to Text Recall@5 [%]

## 4 EVALUATION

We have evaluated the performance of `jina-clip-v2` on a selection of benchmarks: English and multilingual cross-modal retrieval benchmarks in Section 4.1, common text embedding tasks from the MTEB benchmark suite in Section 4.2, visual document retrieval tasks in Section 4.3, and an ablation study of `jina-clip-v2`’s matryoshka representations in Section 4.4.

Detailed evaluation results are presented in the appendices. Detailed CLIP Benchmark results are given in Appendix tables 7, 8 and 9, MTEB results are in Appendix 10. ViDoRe benchmark results are in Appendix 11. A full MRL evaluation can be found in tables 12, 13, 14, 15 in the appendices.

### 4.1 CROSS-MODAL EVALUATION

We evaluate `jina-clip-v2` on a set of English and multilingual cross-modal tasks, conducting a comparative analysis against both its predecessor `jina-clip-v1` and the NLLB-CLIP-SigLIP (Visheratin, 2023b) large and base variants, a top-performing multilingual CLIP model. Additionally, we track the model’s performance at different training stages to evaluate the effectiveness of different parts of the training protocol. Measuring 865M parameters, our model sits between the two NLLB-CLIP-SigLIP versions in terms of size: `nllb-siglip-base` (507M parameters, 41% smaller than ours) and `nllb-siglip-large` (1.2B parameters, 39% larger than ours).

For English zero-shot image-text and text-image retrieval, we conduct evaluations on Flickr30K (Young et al., 2014) and MS COCO Captions (Chen et al., 2015), both of which are included in the CLIP Benchmark. For multilingual cross-modal tasks, we assess performance on the Crossmodal-3600 (Thapliyal et al., 2022) and multilingual MS COCO (Chen et al., 2015) datasets.

As shown in Table 2, `jina-clip-v2` demonstrates strong performance across both English and multilingual benchmarks while showing clear progression through its training stages. On the English CLIP Benchmark, the final model achieves 79.09% and 89.73% on text-to-image and image-to-text retrieval respectively, showing significant improvement from stage 1’s 73.87% and 86.61%. While `nllb-siglip-large` leads in text-to-image retrieval at 81.54%, `jina-clip-v2` outperforms its predecessor `jina-clip-v1` and surpasses both NLLB-CLIP-SigLIP variants in image-to-text retrieval by 2.1% and 1.6% respectively. On the multilingual front, we obtain competitive results on Crossmodal-3600, achieving 81.43% and 83.23% on text-to-image and image-to-text retrieval respectively, approaching the performance of `nllb-siglip-large`. On multilingual MS COCO (Chen et al., 2015), `jina-clip-v2` performs comparably to NLLB-CLIP-SigLIP models, reaching 84.87% and 86.03% on text-to-image and image-to-text retrieval. The improvement from Stage 1 to the final model is notable across all benchmarks, with gains of up to 10.6 percentage points on Crossmodal-3600’s text-to-image retrieval, demonstrating the effectiveness of the training strategy.

### 4.2 TEXT RETRIEVAL AND STS EVALUATION

Table 3 presents the evaluation on MTEB tasks, demonstrating the effectiveness of `jina-clip-v2`’s text encoder for both retrieval and semantic textual similarity (STS) tasks.

Table 3: Evaluation results on MTEB tasks

Benchmark	Retrieval		STS	
	Metric		Spearman Correlation [%]	
Model - Language	EN	Multilingual	EN	Multilingual
nllb-siglip-large	24.91	-	74.89	-
jina-embeddings-v3	<b>53.87</b>	<b>72.58</b>	<b>85.80</b>	<b>69.81</b>
jina-clip-v1	48.33	-	80.92	-
jina-clip-v2stage 1	40.91	-	79.67	-
jina-clip-v2stage 2	43.17	-	80.33	-
jina-clip-v2	49.32	69.85	81.29	67.77

On English retrieval tasks (nDCG@10), `jina-clip-v2` achieves an average score of 49.32, a significant improvement over `nllb-siglip-large`'s 24.91 and a slight improvement over `jina-clip-v1`'s 48.33, though not reaching `jina-embeddings-v3`'s score of 53.87. For multilingual retrieval, the model achieves 69.85, approaching `jina-embeddings-v3`'s performance of 72.58. In STS tasks measured by Spearman Correlation, `jina-clip-v2` demonstrates competitive performance with 81.29 for English tasks, surpassing `nllb-siglip-large`'s 74.89 and comparable to `jina-clip-v1`'s 80.92, though below `jina-embeddings-v3`'s 85.8. On multilingual STS tasks, the model achieves 67.77, slightly below `jina-embeddings-v3`'s 69.8.

### 4.3 VISUAL DOCUMENT RETRIEVAL

Table 4: ViDoRe benchmark performance summary

Model	Average (nDCG@5) [%]
<code>jina-clip-v1</code>	17.72
<code>nllb-siglip-large</code>	46.55
<code>jina-clip-v2</code>	<b>52.65</b>
<code>jina-clip-v2stage 1</code>	37.37
<code>jina-clip-v2stage 2</code>	47.76

Visual document retrieval requires vision models to capture fine-grained information from images to accurately match documents with queries. This task is particularly challenging as it deals with high-resolution document images, which differ significantly from typical image-caption datasets. As shown in table 4, `jina-clip-v2` achieves state-of-the-art performance on the ViDoRe Benchmark (Faysse et al., 2024) for visual document understanding, with an average nDCG@5 score of 52.65%, significantly outperforming both its predecessor `jina-clip-v1` (17.72%) and `nllb-siglip-large` (46.55%). The progression through training stages demonstrates substantial improvements, advancing from 37.37% in stage 1 to 47.76% in stage 2, before reaching peak performance in the final model. These results highlight the effectiveness of our training strategy and the impact of the new datasets introduced for document retrieval tasks.

### 4.4 MATRYOSHKA REPRESENTATION LEARNING

Table 5 presents the impact of embedding truncation on the performance of our model. The table is divided into 4 task categories: text-to-image retrieval, image-to-text retrieval, text-to-text retrieval and semantic textual similarity (STS).

The results show that performance remains highly stable when reducing dimensions from 1024 to 256, with minimal degradation (typically less than 1%) across all evaluation tasks. At 256 dimensions, representing a 75% reduction in embedding size, the model effectively preserves essential semantic information. Substantial performance degradation is only observed at very low dimensions (128 and 64), indicating the model's very robust acquisition of image and text features.

Table 5: MRL ablation study on various embedding dimensions

Dataset - Dimension	1024	768	512	256	128	64
<b>Text-Image Retrieval - Recall@5 [%]</b>						
Avg CLIP Benchmark	79.10	<b>79.12</b>	78.93	78.32	75.90	70.51
Avg Crossmodal-3600	81.43	<b>82.35</b>	82.31	81.75	78.17	72.52
Avg Multilingual MS COCO	<b>84.87</b>	84.85	84.60	84.32	81.80	77.85
<b>Image-Text Retrieval - Recall@5 [%]</b>						
Avg CLIP Benchmark	<b>89.73</b>	89.60	89.55	89.35	87.48	83.20
Avg Crossmodal-3600	83.23	<b>83.26</b>	83.21	82.81	80.54	75.37
Avg Multilingual MS COCO	<b>86.03</b>	86.02	86.02	85.84	84.37	81.02
<b>Text-Text Retrieval - nDCG@10 [%]</b>						
Avg Retrieval	<b>49.33</b>	49.32	49.19	48.67	46.37	40.66
<b>Semantic Textual Similarity - Spearman Correlation [%]</b>						
Avg STS	<b>81.29</b>	81.27	81.26	81.24	80.78	79.56

## 5 ANALYSIS

### 5.1 THE ROLE OF IMAGE RESOLUTION IN COMPLEX DOCUMENT RETRIEVAL

Our empirical study demonstrates that image resolution plays a critical role in retrieving visually rich documents. To better understand the relationship between image resolution and model performance on such documents, we have conducted a targeted experiment.

We checkpointed `jina-clip-v2` at the end of Stage 1, when it had only seen images with a resolution of (224, 224). This model checkpoint was trained on 1.45 billion image-caption pairs and 1.45 billion text-text pairs. We conducted four runs, keeping the image resolution to (224, 224) for the first run and increasing to (384, 384), (512, 512), and (768, 768) for three additional runs. Each run is trained for 3500 steps using the same visually rich training set and hyperparameters. The models are then evaluated on the ViDoRe benchmark (Faysse et al., 2024), which comprises 10 datasets designed for retrieving visually rich documents, based on text queries.

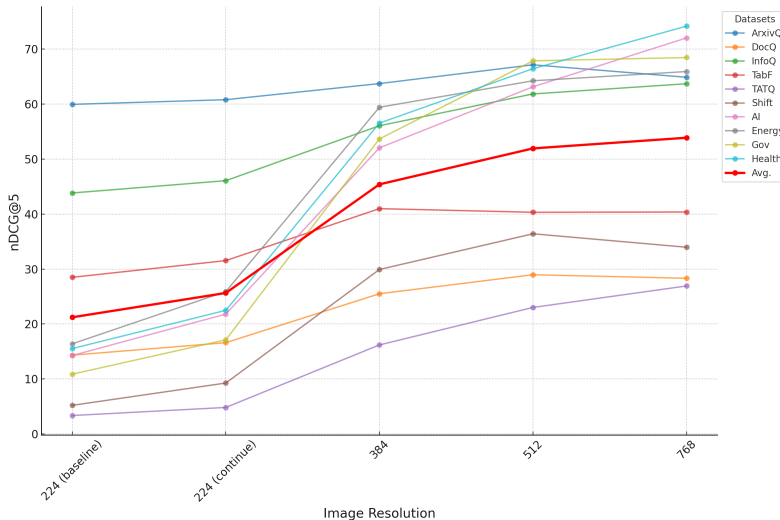


Figure 2: Model performance on the ViDoRe benchmark (Faysse et al., 2024) against input resolution



We have plotted the results in Figure 2. Unsurprisingly, increasing image resolution has a positive impact on linking captions to visually rich documents. The most significant improvement occurs when resolution increases from (224, 224) to (384, 384), with the average nDCG@5 score across 10 benchmarks rising from 0.256 to 0.454. A further increase in resolution to (512, 512) also brings a noticeable gain in performance.

Considering that the model is trained with a patch size of 14, increasing the resolution beyond (512, 512) significantly raises the number of patches, a 2.25x increase when moving from (512, 512) to (768, 768). This leads to substantial additional computational overhead while yielding only marginal improvement, with nDCG@5 increasing by just 0.019. Therefore, we identify (512, 512) as an optimal image resolution, offering a good balance between performance and computational efficiency.

## 5.2 UNIFIED BATCH VS MULTI-TASK LEARNING

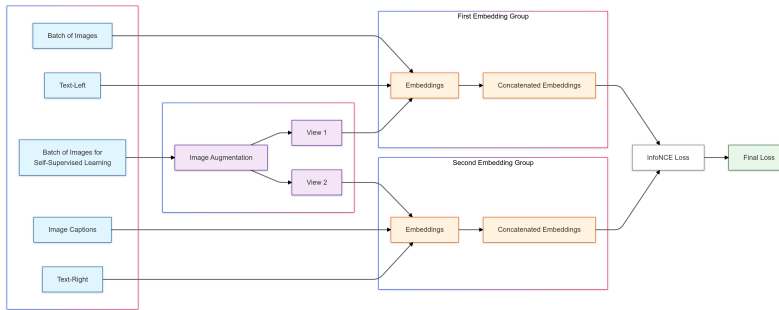


Figure 3: The Unified Batch technique. Contrastive learning between two embedding groups. The first group concatenates original images, question texts, and one view of augmented images, while the second group concatenates corresponding image captions, answer texts, and a different view of the augmented images. These concatenated embeddings are contrasted using the InfoNCE (Van den Oord et al., 2018) loss.

Our training approach, as outlined in Section 3, involves two tasks at each stage, both optimized in a multi-task learning framework: a multi-modal alignment task for images and text, and second text-only task. Both use the InfoNCE (Van den Oord et al., 2018) objective. Regardless of whether the loss is computed on image-text or text-text pairs, the same loss function is applied to pairs of vectors. This raises the question: Would unifying the two batches of pairs into a single batch, irrespective of modality, and optimizing a single contrastive objective, offer any benefits?

We refer to this approach as the unified batch technique, in contrast to the multi-task learning paradigm. We present the training paradigm in Figure 3. The motivation is two-fold: first, simplicity of computation and secondly, modality gap mitigation (Liang et al., 2022) by using in-batch negatives across modalities. Compared to multi-task training, the unified batch approach utilizes a single InfoNCE loss with a shared temperature value, attempting to force all modalities to align within the same embedding space. Additionally, we integrate a SimCLR-like self-supervised learning method (Chen et al., 2020) into the contrastive training, aiming to provide more robust image representation.

However, our Stage 1 experiments show that this technique does bring some early improvements, but fails beyond a certain point, at least with regard to cross-modal tasks. This was reflected in the slow decay of the loss temperature  $\tau$  (our temperature is a trainable parameter in this case) and its eventual stabilization around 0.02. This is in contrast to the multi-task learning approach, where the temperature value decreases more rapidly and keeps decreasing throughout training, leading to better performance on cross-modal tasks.

We hypothesize that this limitation arises from the fundamental information asymmetry between the visual and textual modalities (Schrodi et al., 2024). Images include fine-grained details of information whereas the corresponding textual descriptions include more coarse-grained level of information (Schrodi et al., 2024; Chen et al., 2023b). In temperature-scaled contrastive learning,

---

the temperature parameter controls the hardness of the loss function with respect to the negative samples, i.e., the level of penalties on the hard negative samples (Wang & Liu, 2021). From an information-theory perspective, the level of penalty on the hard negative text-text samples theoretically differs from that of image-text samples due to the information gap problem. Consequently, as supported by our experiments, enforcing a unified temperature parameter across both modalities is potentially theoretically suboptimal.

## 6 CONCLUSION

In this work we present an enhanced strategy for training dual-encoder vision-language embedding models for cross-modal and text retrieval tasks, using contrastive learning. We introduce improvements to the pipeline, namely support for multiple languages, Matryoshka Representation Learning, and finer visual perception. We have trained and released a new model, `jina-clip-v2`, which has strong cross-modal and text retrieval performance on standard benchmarks. Finally, we have conducted analyses of three important considerations for CLIP models going forward: the ability to understand complex visual inputs performance how the image resolution affects it, and the effects of efforts to mitigate the modality gap.

## REFERENCES

- Fredrik Carlsson, Philipp Eisen, Faton Rekathati, and Magnus Sahlgren. Cross-lingual and multi-lingual clip. In *Proceedings of the thirteenth language resources and evaluation conference*, pp. 6848–6854, 2022.
- Jianlv Chen, Shitao Xiao, Peitian Zhang, Kun Luo, Defu Lian, and Zheng Liu. Bge m3-embedding: Multi-lingual, multi-functionality, multi-granularity text embeddings through self-knowledge distillation. *arXiv preprint arXiv:2402.03216*, 2024.
- Lin Chen, Jinsong Li, Xiaoyi Dong, Pan Zhang, Conghui He, Jiaqi Wang, Feng Zhao, and Dahua Lin. Sharegpt4v: Improving large multi-modal models with better captions, 2023a. URL <https://arxiv.org/abs/2311.12793>.
- Ting Chen, Simon Kornblith, Mohammad Norouzi, and Geoffrey Hinton. A simple framework for contrastive learning of visual representations. In *International conference on machine learning*, pp. 1597–1607. PMLR, 2020.
- Weijing Chen, Linli Yao, and Qin Jin. Rethinking benchmarks for cross-modal image-text retrieval. In *Proceedings of the 46th International ACM SIGIR Conference on Research and Development in Information Retrieval, SIGIR '23*, pp. 1241–1251, New York, NY, USA, 2023b. Association for Computing Machinery. ISBN 9781450394086. doi: 10.1145/3539618.3591758. URL <https://doi.org/10.1145/3539618.3591758>.
- Xinlei Chen, Hao Fang, Tsung-Yi Lin, Ramakrishna Vedantam, Saurabh Gupta, Piotr Dollár, and C. Lawrence Zitnick. Microsoft COCO Captions: Data Collection and Evaluation Server. *arXiv preprint arXiv:1504.00325*, 2015. URL <http://arxiv.org/abs/1504.00325>.
- Alexis Conneau, Kartikay Khandelwal, Naman Goyal, Vishrav Chaudhary, Guillaume Wenzek, Francisco Guzmán, Edouard Grave, Myle Ott, Luke Zettlemoyer, and Veselin Stoyanov. Un-supervised cross-lingual representation learning at scale, 2020. URL <https://arxiv.org/abs/1911.02116>.
- Marta R Costa-jussà, James Cross, Onur Çelebi, Maha Elbayad, Kenneth Heafield, Kevin Heffernan, Elahe Kalbassi, Janice Lam, Daniel Licht, Jean Maillard, et al. No language left behind: Scaling human-centered machine translation. *arXiv preprint arXiv:2207.04672*, 2022.
- Tri Dao, Daniel Y. Fu, Stefano Ermon, Atri Rudra, and Christopher Ré. Flashattention: Fast and memory-efficient exact attention with io-awareness, 2022. URL <https://arxiv.org/abs/2205.14135>.
- Alex Fang, Albin Madappally Jose, Amit Jain, Ludwig Schmidt, Alexander Toshev, and Vaishaal Shankar. Data filtering networks, 2023a. URL <https://arxiv.org/abs/2309.17425>.

- 
- Yuxin Fang, Quan Sun, Xinggang Wang, Tiejun Huang, Xinlong Wang, and Yue Cao. EVA-02: A Visual Representation for Neon Genesis. *arXiv preprint arXiv:2303.11331*, 2023b. URL <https://arxiv.org/abs/2303.11331>.
- Manuel Faysse, Hugues Sibille, Tony Wu, Bilel Omrani, Gautier Viaud, Céline Hudelot, and Pierre Colombo. Colpali: Efficient document retrieval with vision language models, 2024. URL <https://arxiv.org/abs/2407.01449>.
- Samir Yitzhak Gadre, Gabriel Ilharco, Alex Fang, Jonathan Hayase, Georgios Smyrnis, Thao Nguyen, Ryan Marten, Mitchell Wortsman, Dhruva Ghosh, Jieyu Zhang, Eyal Orgad, Rahim Entezari, Giannis Daras, Sarah Pratt, Vivek Ramanujan, Yonatan Bitton, Kalyani Marathe, Stephen Mussmann, Richard Vencu, Mehdi Cherti, Ranjay Krishna, Pang Wei Koh, Olga Saukh, Alexander Ratner, Shuran Song, Hannaneh Hajishirzi, Ali Farhadi, Romain Beaumont, Sewoong Oh, Alex Dimakis, Jenia Jitsev, Yair Carmon, Vaishaal Shankar, and Ludwig Schmidt. Datacomp: In search of the next generation of multimodal datasets, 2023. URL <https://arxiv.org/abs/2304.14108>.
- Edward J. Hu, Yelong Shen, Phillip Wallis, Zeyuan Allen-Zhu, Yuanzhi Li, Shean Wang, Lu Wang, and Weizhu Chen. Lora: Low-rank adaptation of large language models, 2021. URL <https://arxiv.org/abs/2106.09685>.
- Albert Q Jiang, Alexandre Sablayrolles, Arthur Mensch, Chris Bamford, Devendra Singh Chaplot, Diego de las Casas, Florian Bressand, Gianna Lengyel, Guillaume Lample, Lucile Saulnier, et al. Mistral 7b. *arXiv preprint arXiv:2310.06825*, 2023.
- Andreas Koukounas, Georgios Mastrapas, Michael Günther, Bo Wang, Scott Martens, Isabelle Mohr, Saba Sturua, Mohammad Kalim Akram, Joan Fontanals Martínez, Saahil Ognawala, Susana Guzman, Maximilian Werk, Nan Wang, and Han Xiao. Jina clip: Your clip model is also your text retriever, 2024. URL <https://arxiv.org/abs/2405.20204>.
- Aditya Kusupati, Gantavya Bhatt, Aniket Rege, Matthew Wallingford, Aditya Sinha, Vivek Ramanujan, William Howard-Snyder, Kaifeng Chen, Sham Kakade, Prateek Jain, and Ali Farhadi. Matryoshka representation learning, 2024. URL <https://arxiv.org/abs/2205.13147>.
- Benjamin Lefaudeux, Francisco Massa, Diana Liskovich, Wenhan Xiong, Vittorio Caggiano, Sean Naren, Min Xu, Jieru Hu, Marta Tintore, Susan Zhang, Patrick Labatut, Daniel Haziza, Luca Wehrstedt, Jeremy Reizenstein, and Grigory Sizov. xformers: A modular and hackable transformer modelling library. <https://github.com/facebookresearch/xformers>, 2022.
- Lei Li, Yuqi Wang, Runxin Xu, Peiyi Wang, Xiachong Feng, Lingpeng Kong, and Qi Liu. Multimodal ArXiv: A dataset for improving scientific comprehension of large vision-language models. In Lun-Wei Ku, Andre Martins, and Vivek Srikumar (eds.), *Proceedings of the 62nd Annual Meeting of the Association for Computational Linguistics (Volume 1: Long Papers)*, pp. 14369–14387, Bangkok, Thailand, August 2024. Association for Computational Linguistics. doi: 10.18653/v1/2024.acl-long.775. URL <https://aclanthology.org/2024.acl-long.775>.
- Shengzhi Li and Nima Tajbakhsh. Scigraphqa: A large-scale synthetic multi-turn question-answering dataset for scientific graphs, 2023. URL <https://arxiv.org/abs/2308.03349>.
- Weixin Liang, Yuhui Zhang, Yongchan Kwon, Serena Yeung, and James Zou. Mind the gap: Understanding the modality gap in multi-modal contrastive representation learning, 2022. URL <https://arxiv.org/abs/2203.02053>.
- Sheng-Chieh Lin, Chankyu Lee, Mohammad Shoeybi, Jimmy Lin, Bryan Catanzaro, and Wei Ping. Mm-embed: Universal multimodal retrieval with multimodal llms, 2024. URL <https://arxiv.org/abs/2411.02571>.
- Ilya Loshchilov and Frank Hutter. Decoupled weight decay regularization, 2019. URL <https://arxiv.org/abs/1711.05101>.

- 
- Minesh Mathew, Viraj Bagal, Rubèn Pérez Tito, Dimosthenis Karatzas, Ernest Valveny, and C. V Jawahar. Infographicvqa, 2021a. URL <https://arxiv.org/abs/2104.12756>.
- Minesh Mathew, Dimosthenis Karatzas, and C. V. Jawahar. Docvqa: A dataset for vqa on document images, 2021b. URL <https://arxiv.org/abs/2007.00398>.
- Niklas Muennighoff, Nouamane Tazi, Loïc Magne, and Nils Reimers. Mteb: Massive text embedding benchmark, 2023. URL <https://arxiv.org/abs/2210.07316>.
- OpenAI. Gpt-4v(ision) system card, 2023. URL <https://api.semanticscholar.org/CorpusID:263218031>.
- Alec Radford, Jong Wook Kim, Chris Hallacy, Aditya Ramesh, Gabriel Goh, Sandhini Agarwal, Girish Sastry, Amanda Askell, Pamela Mishkin, Jack Clark, Gretchen Krueger, and Ilya Sutskever. Learning transferable visual models from natural language supervision, 2021. URL <https://arxiv.org/abs/2103.00020>.
- Simon Schrodi, David T Hoffmann, Max Argus, Volker Fischer, and Thomas Brox. Two effects, one trigger: On the modality gap, object bias, and information imbalance in contrastive vision-language representation learning. *arXiv preprint arXiv:2404.07983*, 2024.
- Krishna Srinivasan, Karthik Raman, Jiecao Chen, Michael Bendersky, and Marc Najork. Wit: Wikipedia-based image text dataset for multimodal multilingual machine learning. *arXiv preprint arXiv:2103.01913*, 2021.
- Saba Sturua, Isabelle Mohr, Mohammad Kalim Akram, Michael Günther, Bo Wang, Markus Krimmel, Feng Wang, Georgios Mastrapas, Andreas Koukounas, Nan Wang, and Han Xiao. jina-embeddings-v3: Multilingual embeddings with task lora, 2024. URL <https://arxiv.org/abs/2409.10173>.
- Jianlin Su, Yu Lu, Shengfeng Pan, Ahmed Murtadha, Bo Wen, and Yunfeng Liu. Roformer: Enhanced transformer with rotary position embedding, 2023. URL <https://arxiv.org/abs/2104.09864>.
- Quan Sun, Yuxin Fang, Ledell Wu, Xinlong Wang, and Yue Cao. Eva-clip: Improved training techniques for clip at scale, 2023. URL <https://arxiv.org/abs/2303.15389>.
- Ashish Thapliyal, Jordi Pont-Tuset, Xi Chen, and Radu Soricut. Crossmodal-3600: A Massively Multilingual Multimodal Evaluation Dataset. In *EMNLP*, 2022.
- A. Van den Oord, Yazhe Li, and Oriol Vinyals. Representation Learning with Contrastive Predictive Coding. *arXiv preprint arXiv:1807.03748*, 2018. URL <http://arxiv.org/abs/1807.03748>.
- Alexander Visheratin. Nllb-clip—train performant multilingual image retrieval model on a budget. *arXiv preprint arXiv:2309.01859*, 2023a.
- Alexander Visheratin. Nllb-clip – train performant multilingual image retrieval model on a budget, 2023b. URL <https://arxiv.org/abs/2309.01859>.
- Feng Wang and Huaping Liu. Understanding the behaviour of contrastive loss. In *2021 IEEE/CVF Conference on Computer Vision and Pattern Recognition (CVPR)*, pp. 2495–2504, 2021. doi: 10.1109/CVPR46437.2021.00252.
- Liang Wang, Nan Yang, Xiaolong Huang, Linjun Yang, Rangan Majumder, and Furu Wei. Multilingual e5 text embeddings: A technical report. *arXiv preprint arXiv:2402.05672*, 2024.
- Peter Young, Alice Lai, Micah Hodosh, and Julia Hockenmaier. From image descriptions to visual denotations: New similarity metrics for semantic inference over event descriptions. *Transactions of the Association for Computational Linguistics*, 2:67–78, 2014. doi: 10.1162/tacl.a.00166. URL <https://aclanthology.org/Q14-1006>.
- Xiaohua Zhai, Xiao Wang, Basil Mustafa, Andreas Steiner, Daniel Keysers, Alexander Kolesnikov, and Lucas Beyer. Lit: Zero-shot transfer with locked-image text tuning. In *Proceedings of the IEEE/CVF conference on computer vision and pattern recognition*, pp. 18123–18133, 2022.

- 
- Xiaohua Zhai, Basil Mustafa, Alexander Kolesnikov, and Lucas Beyer. Sigmoid loss for language image pre-training, 2023. URL <https://arxiv.org/abs/2303.15343>.
- Beichen Zhang, Pan Zhang, Xiaoyi Dong, Yuhang Zang, and Jiaqi Wang. Long-clip: Unlocking the long-text capability of clip, 2024a. URL <https://arxiv.org/abs/2403.15378>.
- Xin Zhang, Yanzhao Zhang, Dingkun Long, Wen Xie, Ziqi Dai, Jialong Tang, Huan Lin, Baosong Yang, Pengjun Xie, Fei Huang, et al. mgte: Generalized long-context text representation and reranking models for multilingual text retrieval. *arXiv preprint arXiv:2407.19669*, 2024b.
- Fengbin Zhu, Wenqiang Lei, Fuli Feng, Chao Wang, Haozhou Zhang, and Tat-Seng Chua. Towards complex document understanding by discrete reasoning. In *Proceedings of the 30th ACM International Conference on Multimedia*, MM '22, pp. 4857–4866. ACM, October 2022. doi: 10.1145/3503161.3548422. URL <http://dx.doi.org/10.1145/3503161.3548422>.

A APPENDIX

Table 6: Training settings on each stage

Parameter	Stage 1	Stage 2	Stage 3
Image encoder weights init	EVA02 ViT L/14 (Sun et al., 2023)	Stage 1	Stage 2
Text encoder weights init	JinaXLMRoBERTa (Sturua et al., 2024)	Stage 1	Stage 2
Peak image encoder LR	2e-4	5e-5	5e-6
Image encoder layer-wise LR decay	1	0.98	1
Peak text encoder LR	1e-4	5e-5	1e-4
Text encoder layer-wise LR decay	1	0.98	1
Image-text pairs batch size	16,384	8,192	1,024
Text pairs batch size	16,384	8,192	128
Total steps	100,000	6,000	16,000
Max sequence length	77	512	512
Image-text pairs samples seen	1.7B	50M	16M
Text pairs samples seen	1.7B	50M	2M
Number of GPUs - H100s 80GB	8	8	8
LR schedule	cosine decay		
Optimizer	AdamW (Loshchilov & Hutter, 2019)		
Optimizer hyper-parameters	$\beta_1, \beta_2, \epsilon = 0.9, 0.98, 1e - 6$		
Weight decay	0.02		
Input resolution	(224...384, 224...384)	(384, 384)	(512, 512)
Patch size	(14, 14)		
Numerical precision	bfloat16		

Table 7: Model performance on the CLIP Benchmark retrieval tasks

Dataset - Model	jina-clip-v2	jina-clip-v2 stage 1	jina-clip-v2 stage 2	jina-clip-v1	nllb-siglip large	nllb-siglip base
<b>Zero-shot Image Retrieval - Recall@5 [%]</b>						
Flickr30K (Young et al., 2014)	89.84	86.84	90.04	89.04	<b>92.24</b>	90.02
MS COCO (Chen et al., 2015)	68.35	60.91	69.59	66.42	<b>70.84</b>	69.13
<b>Zero-shot Text Retrieval - Recall@5 [%]</b>						
Flickr30K (Young et al., 2014)	<b>98.00</b>	96.10	97.40	96.40	97.10	95.00
MS COCO (Chen et al., 2015)	81.46	77.12	<b>81.74</b>	79.02	79.20	77.76

Table 8: Model performance on Crossmodal-3600 (Thapliyal et al., 2022)

Language - Model	jina-clip-v2	jina-clip-v2 stage 1	jina-clip-v2 stage 2	nllb-siglip large	nllb-siglip base
<b>Zero-shot Image Retrieval - Recall@5 [%]</b>					
<b>average</b>	81.43	73.51	<b>84.13</b>	82.07	79.29
ar	73.56	66.22	76.89	<b>78.92</b>	76.94
bn	63.78	50.19	68.11	<b>75.19</b>	74.19
da	85.39	76.53	<b>87.97</b>	87.14	86.64
de	91.25	84.64	<b>92.42</b>	89.56	87.25
el	75.03	68.53	<b>77.92</b>	77.83	71.97
en	75.83	69.78	<b>77.78</b>	73.11	72.22
es	83.64	78.28	<b>86.28</b>	82.64	79.97
fi	82.83	75.28	85.89	<b>86.42</b>	81.44
fr	88.78	83.50	<b>90.67</b>	87.86	85.58
hi	55.25	42.03	59.47	<b>60.31</b>	58.08
id	84.22	73.69	<b>86.94</b>	86.31	84.17
it	88.33	81.19	<b>89.64</b>	85.94	82.67
ja	87.03	77.28	<b>90.03</b>	86.06	83.14
ko	78.81	71.81	<b>83.22</b>	78.75	75.47
nl	82.56	75.72	<b>84.47</b>	81.69	78.86
no	81.08	71.97	<b>83.08</b>	82.69	79.97
pl	84.00	79.33	<b>86.50</b>	82.72	78.61
pt	82.42	76.17	<b>85.19</b>	82.69	79.44
ro	89.36	82.92	<b>92.22</b>	90.03	86.17
ru	88.97	82.97	<b>91.11</b>	86.44	83.78
sv	78.06	71.33	<b>80.56</b>	79.33	76.17
th	81.61	70.92	<b>85.08</b>	81.14	78.83
tr	81.31	75.31	<b>84.53</b>	83.47	81.00
uk	88.56	82.28	<b>89.89</b>	85.44	81.89
vi	86.64	76.31	<b>89.06</b>	85.56	82.56
zh	78.97	66.97	<b>82.50</b>	76.56	74.64
<b>Zero-shot Text Retrieval - Recall@5 [%]</b>					
<b>average</b>	83.23	79.64	<b>84.12</b>	80.16	76.56
ar	76.25	72.14	<b>76.67</b>	75.86	73.69
bn	69.00	63.78	70.22	<b>75.58</b>	73.61
da	88.53	84.42	<b>88.86</b>	86.53	84.69
de	<b>92.47</b>	88.42	<b>92.47</b>	87.50	84.44
el	73.33	73.22	<b>75.61</b>	74.81	68.89
en	78.58	74.33	<b>79.61</b>	70.81	69.08
es	86.28	81.19	<b>87.36</b>	81.19	77.00
fi	84.19	81.17	<b>85.64</b>	84.25	78.75
fr	90.89	86.56	<b>91.00</b>	86.64	83.64
hi	61.64	54.39	61.56	<b>61.89</b>	59.83
id	86.31	83.64	<b>87.64</b>	84.33	81.89
it	90.17	84.31	<b>90.53</b>	83.50	78.64
ja	88.50	85.53	<b>89.44</b>	84.03	81.14
ko	81.42	79.22	<b>83.00</b>	76.75	74.17
nl	82.47	77.94	<b>83.33</b>	79.28	74.33
no	83.75	77.22	<b>84.42</b>	82.08	77.03
pl	84.61	83.72	<b>85.69</b>	79.58	75.39
pt	83.94	79.31	<b>84.06</b>	79.39	74.89
ro	91.31	87.39	<b>92.08</b>	88.83	83.58
ru	90.64	87.75	<b>90.89</b>	84.64	80.61
sv	78.28	77.53	<b>80.11</b>	76.58	72.31
th	81.94	80.22	<b>84.11</b>	79.56	76.28
tr	82.67	80.36	<b>83.81</b>	80.36	77.69
uk	89.53	86.42	<b>89.97</b>	83.22	78.67
vi	88.06	85.64	<b>88.58</b>	83.14	80.03
zh	79.22	74.94	<b>80.42</b>	73.83	70.22

Table 9: Model performance on multilingual MS COCO (Chen et al., 2015)

Language - Model	jina-clip-v2	jina-clip-v2 stage 1	jina-clip-v2 stage 2	nllb-siglip large	nllb-siglip base
<b>Zero-shot Image Retrieval - Recall@5 [%]</b>					
<b>average</b>	84.87	80.66	86.11	<b>87.60</b>	86.23
de	85.70	80.40	86.80	<b>88.30</b>	87.00
en	<b>89.40</b>	84.00	<b>89.40</b>	<b>89.40</b>	88.80
es	85.90	82.70	87.40	<b>88.20</b>	86.70
fr	85.10	80.90	87.30	<b>87.70</b>	86.90
it	85.80	83.20	87.10	<b>89.30</b>	87.80
ko	82.10	78.30	83.00	<b>85.20</b>	83.60
pl	86.50	81.10	88.00	<b>89.40</b>	87.60
ru	81.10	79.30	82.10	<b>83.40</b>	82.40
tr	83.70	81.30	86.30	<b>88.30</b>	86.80
zh	83.40	75.40	83.70	<b>86.80</b>	84.70
<b>Zero-shot Text Retrieval - Recall@5 [%]</b>					
<b>average</b>	86.03	83.02	<b>86.45</b>	85.37	84.56
de	86.20	82.90	<b>86.90</b>	84.40	84.30
en	90.50	87.80	<b>90.60</b>	88.30	87.50
es	87.00	84.90	<b>87.50</b>	85.80	85.20
fr	85.20	82.20	85.00	<b>86.30</b>	84.40
it	<b>88.00</b>	83.10	87.70	86.70	85.60
ko	82.10	79.30	<b>84.00</b>	83.20	82.60
pl	88.50	84.50	<b>88.90</b>	86.80	86.60
ru	<b>83.10</b>	79.60	81.80	80.90	81.20
tr	85.60	83.20	85.90	<b>87.10</b>	85.40
zh	84.10	82.70	<b>86.20</b>	84.20	82.80



Table 10: Model performance on MTEB (Muennighoff et al., 2023) Retrieval and STS tasks

Dataset - Model	jina-clip-v2	jina-embeddings-v3	jina-clip-v2 stage 1	jina-clip-v2 stage 2	nllb-siglip large	jina-clip-v1
<b>Retrieval - nDCG@10</b>						
<b>Average Retrieval</b>	49.33	<b>53.87</b>	40.91	43.17	24.92	48.33
ArguAna	43.55	<b>54.33</b>	41.87	45.84	40.63	49.36
ClimateFEVER	30.12	<b>42.36</b>	19.32	23.74	15.57	24.81
CQADupstackRetrieval	41.20	<b>42.36</b>	41.57	42.09	21.06	40.92
DBPedia	37.44	<b>41.00</b>	22.04	25.48	20.46	36.64
FEVER	84.96	<b>89.05</b>	60.97	66.13	14.98	76.28
FiQA2018	41.93	<b>47.35</b>	41.87	40.97	12.90	38.27
HotpotQA	60.14	<b>64.67</b>	49.28	47.00	22.38	61.89
MSMARCO	37.47	<b>40.82</b>	23.06	27.05	13.35	36.91
NFCorpus	32.89	<b>36.62</b>	30.95	32.11	18.97	33.52
NQ	57.17	<b>64.23</b>	39.78	42.80	16.96	58.09
QuoraRetrieval	88.14	<b>89.09</b>	87.12	86.92	80.71	87.88
SCIDOCS	18.90	19.81	20.51	<b>20.91</b>	10.62	20.24
SciFact	65.34	<b>72.31</b>	68.26	67.61	35.28	67.34
TRECCOVID	76.73	<b>77.72</b>	51.29	58.63	38.15	71.61
Touche2020	23.94	<b>26.30</b>	15.72	20.21	11.75	21.15
<b>STS - Spearman correlation based on cosine similarity</b>						
<b>Average STS</b>	81.29	<b>85.80</b>	79.67	80.33	74.90	80.92
BIOSSES	83.00	<b>88.69</b>	83.55	83.62	65.07	83.75
SICK-R	82.38	<b>89.62</b>	78.96	78.63	75.83	78.95
STS12	76.72	<b>82.43</b>	73.41	74.57	73.60	73.52
STS13	79.90	<b>89.49</b>	80.25	82.35	76.50	83.24
STS14	77.49	<b>84.95</b>	75.13	76.89	76.35	78.68
STS15	86.42	<b>89.31</b>	84.98	85.62	80.90	87.46
STS16	85.18	<b>86.85</b>	83.70	82.66	74.73	83.77
STS17	87.87	<b>89.99</b>	86.13	86.95	83.84	89.77
STS22	67.07	67.28	66.31	<b>67.58</b>	62.52	65.15
STSBenchmark	86.87	<b>89.44</b>	84.27	84.40	79.64	84.93

Table 11: Model performance on the ViDoRe (Faysse et al., 2024) Benchmark

Task	jina-clip-v2	jina-clip-v2 stage 1	jina-clip-v2 stage 2	jina-clip-v1	nllb-siglip large
<b>Retrieval - nDCG@5</b>					
<b>Average</b>	<b>52.65</b>	37.37	47.76	17.72	46.55
ArxivQ	<b>64.92</b>	58.78	66.14	25.40	30.44
DocQ	<b>24.64</b>	21.16	24.81	11.90	23.82
InfoQ	57.90	56.62	56.63	35.50	<b>59.87</b>
TabF	45.91	37.28	43.18	20.20	<b>70.68</b>
TATQ	<b>30.25</b>	12.09	25.79	3.30	20.00
Shift	<b>34.07</b>	28.41	31.54	3.80	30.79
AI	<b>68.07</b>	32.95	55.64	15.20	47.90
Energy	62.15	49.15	60.97	19.70	<b>64.94</b>
Gov	<b>68.97</b>	37.81	55.56	21.40	58.62
Health	<b>69.05</b>	39.50	57.37	20.80	58.43

Table 12: MRL (Kusupati et al., 2024) ablation study on the CLIP Benchmark Retrieval tasks

Dataset - Dimension	1024	768	512	256	128	64
<b>Zero-shot Image Retrieval - Recall@5 [%]</b>						
Flickr30K (Young et al., 2014)	89.84	<b>89.98</b>	89.70	89.20	87.22	81.60
MS COCO (Chen et al., 2015)	<b>68.35</b>	68.26	68.16	67.43	64.58	59.41
<b>Zero-shot Text Retrieval - Recall@5 [%]</b>						
Flickr30K (Young et al., 2014)	98.00	<b>98.10</b>	98.00	98.00	96.30	93.40
MS COCO (Chen et al., 2015)	<b>81.46</b>	81.10	81.10	80.70	78.66	73.00

Table 13: MRL (Kusupati et al., 2024) ablation study on Crossmodal-3600 (Thapliyal et al., 2022)

Language - Dimension	1024	768	512	256	128	64
<b>Zero-shot Image Retrieval - Recall@5 [%]</b>						
<b>average</b>	81.43	<b>82.35</b>	82.31	81.75	78.17	72.52
ar	<b>73.56</b>	73.39	73.17	72.61	68.42	62.28
bn	<b>63.78</b>	63.67	63.64	62.39	57.58	49.58
da	<b>85.39</b>	85.31	84.67	84.53	81.69	75.69
de	91.25	91.28	<b>91.47</b>	<b>91.47</b>	88.75	84.44
el	75.03	75.08	<b>75.25</b>	74.69	72.00	66.81
en	75.83	75.97	<b>76.03</b>	75.72	74.03	69.67
es	83.64	83.67	<b>83.86</b>	83.14	81.00	76.19
fi	82.83	<b>83.03</b>	82.61	81.67	79.44	74.94
fr	<b>88.78</b>	88.75	88.53	88.28	86.92	82.14
hi	<b>55.25</b>	54.97	55.14	54.14	50.06	42.33
id	<b>84.22</b>	84.00	84.11	83.25	80.00	74.17
it	88.33	<b>88.53</b>	88.31	87.83	85.11	79.75
ja	<b>87.03</b>	<b>87.03</b>	86.89	86.33	82.92	75.39
ko	<b>78.81</b>	78.72	78.56	77.03	73.44	65.78
nl	<b>82.56</b>	<b>82.56</b>	82.31	82.25	79.00	73.25
no	<b>81.08</b>	80.94	80.64	80.14	76.94	71.56
pl	84.00	83.97	<b>84.06</b>	83.39	81.28	76.83
pt	82.42	<b>82.50</b>	82.00	81.58	79.36	72.97
ro	89.36	<b>89.39</b>	89.22	89.14	87.03	82.06
ru	88.97	<b>89.17</b>	89.08	88.69	87.00	82.17
sv	<b>78.06</b>	77.86	78.00	77.47	74.83	69.53
th	81.61	<b>81.64</b>	81.14	80.36	76.97	68.17
tr	81.31	<b>81.44</b>	81.22	80.69	77.39	71.33
uk	88.56	88.42	<b>88.61</b>	87.89	85.86	80.72
vi	86.64	<b>86.72</b>	86.69	85.92	83.17	77.86
zh	78.97	<b>79.06</b>	78.86	78.08	74.81	67.36
<b>Zero-shot Text Retrieval - Recall@5 [%]</b>						
<b>average</b>	83.23	<b>83.26</b>	83.21	82.81	80.54	75.37
ar	<b>76.25</b>	76.17	76.17	75.19	73.61	68.25
bn	<b>69.00</b>	<b>69.00</b>	68.94	68.75	66.19	59.39
da	<b>88.53</b>	88.39	88.25	87.58	85.69	80.25
de	92.47	<b>92.56</b>	92.42	92.31	90.64	87.19
el	73.33	<b>73.50</b>	73.47	73.39	72.75	68.61
en	78.58	<b>78.61</b>	78.36	77.86	76.44	72.58
es	86.28	<b>86.39</b>	86.33	85.78	84.03	80.17
fi	84.19	<b>84.25</b>	84.00	83.58	82.08	77.81
fr	<b>90.89</b>	90.86	90.75	90.14	88.61	84.89
hi	<b>61.64</b>	<b>61.64</b>	61.44	61.44	58.86	52.81
id	<b>86.31</b>	86.25	86.19	86.14	83.92	80.19
it	<b>90.17</b>	90.08	<b>90.17</b>	89.83	87.78	83.75
ja	88.50	<b>88.64</b>	<b>88.64</b>	87.92	86.22	81.64
ko	<b>81.42</b>	<b>81.42</b>	81.31	80.53	78.31	73.03
nl	<b>82.47</b>	82.44	82.36	81.94	79.97	76.00
no	83.75	<b>83.81</b>	83.78	83.28	80.39	75.39
pl	84.61	<b>84.67</b>	84.47	83.81	82.36	78.56
pt	<b>83.94</b>	83.83	83.64	83.25	81.72	77.00
ro	<b>91.31</b>	91.14	91.22	91.03	89.44	85.67
ru	<b>90.64</b>	90.58	90.31	90.19	88.50	84.86
sv	<b>78.28</b>	78.22	78.06	77.50	75.97	71.42
th	<b>81.94</b>	81.89	<b>81.94</b>	81.28	79.25	73.61
tr	82.67	<b>82.72</b>	82.39	81.92	80.36	76.06
uk	<b>89.53</b>	<b>89.53</b>	89.31	88.81	88.00	84.69
vi	<b>88.06</b>	87.94	87.61	87.47	85.92	82.00
zh	<b>79.22</b>	79.06	78.83	78.50	76.11	70.22

Table 14: MRL (Kusupati et al., 2024) ablation study on multilingual MS COCO (Chen et al., 2015)

Language - Dimension	1024	768	512	256	128	64
<b>Zero-shot Image Retrieval - Recall@5 [%]</b>						
<b>average</b>	<b>84.87</b>	84.85	84.60	84.32	81.80	77.85
de	<b>85.70</b>	85.40	84.90	84.70	81.10	79.30
en	89.40	<b>89.60</b>	88.70	88.90	86.50	83.00
es	85.90	85.90	<b>86.00</b>	85.70	84.00	80.80
fr	85.10	84.70	84.80	<b>85.30</b>	83.30	79.10
it	85.80	85.50	<b>86.10</b>	85.80	83.70	81.10
ko	<b>82.10</b>	81.90	<b>82.10</b>	80.10	77.90	71.90
pl	86.50	<b>86.70</b>	86.40	86.30	84.80	80.40
ru	81.10	81.20	80.80	<b>81.40</b>	77.80	74.00
tr	83.70	<b>84.10</b>	83.50	83.10	80.00	75.80
zh	83.40	<b>83.50</b>	82.70	81.90	78.90	73.10
<b>Zero-shot Text Retrieval - Recall@5 [%]</b>						
<b>average</b>	<b>86.03</b>	86.02	86.02	85.84	84.37	81.02
de	86.20	<b>86.40</b>	86.10	85.90	85.20	81.50
en	<b>90.50</b>	<b>90.50</b>	91.10	90.40	90.10	86.80
es	<b>87.00</b>	86.80	86.70	86.90	86.10	81.80
fr	<b>85.20</b>	84.90	<b>85.20</b>	85.00	84.20	81.70
it	<b>88.00</b>	<b>88.00</b>	87.70	87.60	85.70	83.20
ko	82.10	82.20	82.40	<b>82.80</b>	80.30	77.50
pl	88.50	<b>88.70</b>	88.60	88.30	85.90	83.60
ru	<b>83.10</b>	83.00	82.70	82.80	80.80	78.10
tr	85.60	85.60	<b>85.90</b>	<b>85.90</b>	84.50	79.80
zh	<b>84.10</b>	<b>84.10</b>	83.80	82.80	80.90	76.20

Table 15: MRL (Kusupati et al., 2024) ablation study on MTEB (Muennighoff et al., 2023) Retrieval and STS tasks

Dataset - Dimensions	1024	768	512	256	128	64
<b>Retrieval - nDCG@10</b>						
<b>Average Retrieval</b>	<b>49.33</b>	49.32	49.19	48.67	46.37	40.66
FiQA2018	41.93	<b>42.04</b>	41.79	40.96	38.75	34.27
NFCorpus	32.89	<b>33.01</b>	32.72	32.32	30.20	25.69
SciFact	<b>65.34</b>	65.12	65.26	64.57	62.51	57.17
SCIDOCs	<b>18.90</b>	18.85	18.84	18.46	16.98	13.84
CQADupstackRetrieval	<b>41.20</b>	41.17	41.06	40.47	37.97	32.42
Touche2020	23.94	24.08	24.23	24.57	<b>25.82</b>	23.26
TRECCOVID	<b>76.73</b>	76.54	75.98	76.01	73.10	67.47
FEVER	84.96	<b>84.99</b>	84.83	84.37	81.40	69.26
HotpotQA	<b>60.14</b>	60.13	59.71	58.06	52.14	38.97
DBPedia	<b>37.44</b>	37.42	36.98	36.12	33.21	26.34
NQ	57.17	<b>57.19</b>	57.02	56.30	53.49	45.42
ClimateFEVER	30.12	30.15	<b>30.35</b>	30.00	26.08	20.89
MSMARCO	<b>37.47</b>	37.43	37.45	37.16	35.74	32.47
ArguAna	<b>43.55</b>	43.50	43.53	42.83	41.06	37.21
QuoraRetrieval	<b>88.14</b>	88.13	88.06	87.88	87.10	85.19
<b>STS - Spearman correlation based on cosine similarity</b>						
<b>Average STS</b>	<b>81.29</b>	81.27	81.26	81.24	80.78	79.56
STS12	76.72	76.72	76.85	76.97	<b>77.13</b>	76.44
STS13	79.90	79.89	79.98	<b>80.48</b>	80.00	78.69
STS14	77.49	77.51	77.57	<b>77.67</b>	77.10	75.50
STS15	86.42	86.43	86.46	<b>86.58</b>	86.21	84.58
STS16	<b>85.18</b>	85.17	85.15	85.10	84.52	84.03
STS17	87.87	<b>87.89</b>	87.74	87.31	86.91	85.36
STS22	<b>67.07</b>	67.04	67.01	66.95	66.66	66.71
BIOSSES	83.00	<b>83.03</b>	82.65	82.33	81.18	78.27
STSBenchmark	<b>86.87</b>	86.68	86.86	86.72	86.26	85.14
SICK-R	<b>82.38</b>	<b>82.38</b>	82.36	82.27	81.87	80.89